

# The performance prediction of roadheaders from easy testing methods

Ergin Kahraman<sup>1</sup> · Sair Kahraman<sup>2</sup>

Received: 20 March 2015 / Accepted: 18 September 2015 / Published online: 3 October 2015  
© Springer-Verlag Berlin Heidelberg 2015

**Abstract** An accurate prediction of roadheader performance helps to make for more efficient and cost effective planning of tunneling projects. In this study, the performance prediction models for roadheaders were developed by using easy testing methods such as Brazilian tensile strength, point load strength, block punch strength, ultrasonic velocity, density, porosity, and the water absorption ratio. A Dosco Mk-2B axial type roadheader has been monitored during roadway construction in an underground lignite mine located in Cayirhan, a town of Ankara and the instantaneous cutting rates (ICR) were calculated. Physical and mechanical tests were conducted on the rock samples collected from each observation location. Simple regression analysis showed that the physico-mechanical rock properties were not correlated with the ICR values. Step-wise multiple regression analysis was also performed, and the best model to predict the ICR of the roadheader was selected. The best model with a high correlation coefficient ( $r = 0.89$ ) includes point load strength and water absorption by weight. The simple models including two variables were also developed for alternative use in practice. In addition, the usability of the derived models in a jointed rock mass was discussed by including a correction factor to the models for geological discontinuities. A concluding remark is that the derived models can be practically used for the estimation of the ICR of roadheaders in similar formations.

**Keywords** Roadheaders · Performance prediction · Indirect tests · Regression analysis

## Introduction

The demand for tunnel and underground spaces has been increasing especially in developed and developing countries. Because the mechanical excavation of rock is faster and more reliable than classical methods, it has been becoming widespread more and more. High advancing rates, flexibility, safety, and optimized operation are the main advantages compared to classical excavation. It also reduces support costs by minimizing break and ground disturbance.

Roadheaders have been widely used in the excavation of soft to medium strength rocks in tunneling and mine developments for about 50 years. They are very flexible and can be used for excavating necessary openings with different size and shape. Having some prior knowledge of the potential performance of a selected roadheader is very important for the planning and cost estimation purposes in rock excavation projects. Several researchers have suggested performance prediction models for roadheaders. These models generally include direct testing methods. In this study, the evaluation of the performance prediction of roadheaders was carried out by using the easy testing methods such as Brazilian tensile strength, point load strength, block punch strength, ultrasonic velocity, density, porosity, and water absorption by weight.

## Previous studies

Specific energy (SE) is a valuable parameter in the mechanical excavation of rock. It can be described as the amount of work required to break a unit volume of rock

✉ Sair Kahraman  
sairkahraman@yahoo.com

<sup>1</sup> Cayirhan Park Thermic Corp., Ankara, Turkey

<sup>2</sup> Mining Engineering Department, Hacettepe University, Ankara, Turkey

and is simply used for the quick performance prediction of roadheaders (Rostami et al. 1994):

$$ICR = k \frac{P}{SE}, \quad (1)$$

where, ICR is the instantaneous cutting rate ( $\text{m}^3/\text{h}$ ),  $P$  is the cutting head power (kW or HP),  $k$  is the energy transfer ratio (0.85–0.90 for TBMs and 0.45–0.55 for roadheaders, and  $SE$  is the specific energy ( $\text{kWh}/\text{m}^3$ ).

Since obtaining  $SE$  from small-scale or full-scale cutting tests is difficult and expensive, some researchers have investigated the relations between  $SE$  and rock properties and suggested empirical equations for the estimation of  $SE$ . McFeat-Smith and Fowell (1979) carried out some experimental studies for correlating the specific energy obtained by small-scale cutting tests for some rock properties such as cone indenter index, cementation coefficient, Schmidt hammer rebound value, and compressive strength. They stated that the cone indenter test consistently proved to be the best predictor for the specific energy prediction. Singh (1987) showed that a directly proportional relation existed between in situ specific energy and brittleness of three Utah coals. Goktan (1991) investigated the relation between  $SE$  and some brittleness concepts and concluded that the brittleness concepts adopted in his study might not be a representative measure of rock cutting specific energy consumption for the studied rocks. Copur et al. (2001) correlated  $SE$  to the uniaxial compressive strength (UCS) and Brazilian tensile strength (BTS) for some rock and ore types. They found good correlation between  $SE$  and both the UCS and BTS. They also showed that the relation between  $SE$  and the product of UCS and BTS has a better correlation coefficient than that of the relations between  $SE$  and both the UCS and BTS, respectively. Altindag (2003) investigated the relations between the  $SE$  and brittleness concepts using the raw data obtained from the previous experimental studies performed on rocks. He showed that the  $SE$  was strongly correlated with the brittleness of  $B_3$  (the area under the line in relation to compressive strength and tensile strength). Balci et al. (2004) tested 23 different rock and ore types and investigated the predictability of  $SE$  from physical and mechanical properties. They found good or strong correlations between the  $SE$  and rock properties such as the uniaxial compressive strength, the Brazilian tensile strength, the static and dynamic elastic modulus, and the Schmidt hammer value. Tiryaki and Dikmen (2006) carried out mineralogical and petrographic analyses, rock mechanics, and linear rock cutting tests on sandstones. They investigated the relations between  $SE$  and rock properties using regression analyses. They showed that the texture coefficient and feldspar content of sandstones affected rock cuttability, evidenced by significant correlations between these parameters and the  $SE$ . However, felsic

and mafic mineral contents of sandstones exhibited no significant correlation with  $SE$ . On the other hand, cementation coefficient, effective porosity, and pore volume indicated good correlations with the  $SE$ . Poisson's ratio, Brazilian tensile strength, Shore scleroscope hardness, Schmidt hammer hardness, dry density, and point load strength index showed very strong linear correlations with  $SE$ . Tumac et al. (2007) investigated the predictability of rock cuttability from Shore hardness and compressive strength. They showed that there was a relation between Shore hardness values, optimum specific energy, and compressive strength. Comakli et al. (2014) investigated the predictability of the excavation capacity of roadheaders for metallic ores and derived some prediction equations for the assessment of specific energy.

In addition to the studies for the prediction of  $SE$  from rock properties, some researchers have developed different models for the prediction of the instantaneous cutting rate of roadheaders. These models are given as follows:

Gehring (1989) presented a performance prediction model based on the performance of a roadheader with a 250 kW transverse type cutterhead:

$$ICR = \frac{719}{\sigma_c^{0.78}}, \quad (2)$$

where ICR is the instantaneous cutting rate of roadheaders ( $\text{m}^3/\text{h}$ ) and  $\sigma_c$  is the uniaxial compressive strength (MPa).

Gehring (1989) also presented a performance prediction model based on the performance of a roadheader with a 230 kW axial type cutterhead:

$$ICR = \frac{1739}{\sigma_c^{1.13}}. \quad (3)$$

Based on the in situ observation of many tunneling and mining projects, Bilgin et al. (1990) suggested a performance prediction model for axial type roadheaders:

$$ICR = 0.28P(0.974)^{RMCI}, \quad (4)$$

$$RMCI = \sigma_c \left( \frac{RQD}{100} \right)^{2/3}, \quad (5)$$

where ICR is the instantaneous cutting rate of roadheaders ( $\text{m}^3/\text{h}$ ),  $P$  is the power of cutting head (HP),  $RMCI$  is the rock mass cuttability index,  $\sigma_c$  is the uniaxial compressive strength (MPa), and RQD is the rock quality designation (%).

Copur et al. (1998) suggested the following model based on extensive field data collected from different roadheader applications in a variety of geologic formations.

$$ICR = 27.511e^{0.0023RPI}, \quad (6)$$

$$RPI = \frac{PW}{\sigma_c}, \quad (7)$$

where ICR is the instantaneous cutting rate of roadheaders ( $m^3/h$ ), RPI is the roadheader penetration index ( $kW \times ton/MPa$ ),  $P$  is the power of cutting head ( $kW$ ),  $W$  is the roadheader weight ( $ton$ ), and  $\sigma_c$  is the uniaxial compressive strength ( $MPa$ ).

Thuro and Plinninger (1999) derived a prediction model based on the performance of a 132 kW transverse type roadheader:

$$ICR = 75.7 - 14.3 \ln \sigma_c, \tag{8}$$

where ICR is the instantaneous cutting rate of roadheaders ( $m^3/h$ ) and  $\sigma_c$  is the uniaxial compressive strength ( $MPa$ ).

Tumac et al. (2007) investigated the relations between the instantaneous cutting rate of a roadheader and Shore hardness and uniaxial compressive strength. They established the following equations:

$$ICR = 81.21SH^{-0.78}, \tag{9}$$

$$ICR = 109.25\sigma_c^{-0.72}, \tag{10}$$

where ICR is the instantaneous cutting rate ( $m^3/h$ ), SH is the Shore hardness, and  $\sigma_c$  is the uniaxial compressive strength ( $MPa$ ).

Ocak and Bilgin (2010) found a good relation between the UCS and the ICR of a roadheader used in Kadikoy–Kartal metro line stations. The equation of the relation is given below:

$$ICR = 510588\sigma_c^{-2.1779}, \tag{11}$$

where ICR is the instantaneous cutting rate ( $m^3/h$ ) and  $\sigma_c$  is the uniaxial compressive strength ( $MPa$ ).

Ebrahimabadi et al. (2011) defined a rock mass brittleness index (RMBI) and found a good relation between ICR and RMBI for roadheaders. The related equations are given as follows:

$$RMBI = e^{(\sigma_c/\sigma_t)x} \left( \frac{RQD}{100} \right)^3, \tag{12}$$

$$ICR = 30.75RMBI^{0.23}, \tag{13}$$

where RMBI is the rock mass brittleness index,  $\sigma_c$  is the uniaxial compressive strength ( $MPa$ ),  $\sigma_t$  is the Brazilian tensile strength ( $MPa$ ), RQD is the rock quality designation of rock mass in per cent, and ICR is the instantaneous cutting rate of roadheaders ( $m^3/h$ ).

Abdolreza and Yakhchali (2013) investigated the predictability of performance of roadheaders from intact and mass properties of rocks and suggested the following equation:

$$ICR = 1.79\sigma_c + 0.501\alpha + 0.636RQD - 4.839\sigma_t - 22.127, \tag{14}$$

where ICR is the instantaneous cutting rate ( $m^3/h$ )  $\sigma_c$  is the uniaxial compressive strength ( $MPa$ ),  $\alpha$  is angle between tunnel axis and the planes of weakness, RQD is the rock quality designation of rock mass (%), and  $\sigma_t$  is the Brazilian tensile strength ( $MPa$ ).

The above listed models include SE or UCS except for Eq. (9). The determination of SE is very difficult and expensive. The carrying out of the UCS test is also tedious, time consuming, and expensive. There may not be sometimes enough samples for the UCS test or getting standard cores for the UCS test may not be possible for some rocks such as weak rock and laminated rocks. For this reason, the development of the performance prediction models including easy and practical test methods will be useful for roadheaders. This study investigates the predictability of roadheader performance by using easy testing methods such as Brazilian tensile strength, point load strength, block punch strength, ultrasonic velocity, density, porosity, and water absorption by weight.

### Study area and geology

The study was carried out in the Cayirhan Lignite Mine located in Cayirhan Town of Nallihan County, 122 km west of Ankara. Figure 1 shows the location map of the Cayirhan Underground Lignite Mine. The mine is operated by the Ciner Group and approximately 5–5.5 million tons of lignite is produced per year. The produced coal is supplied to the Cayirhan Power Plant, which has a 620 MW electricity production capacity.

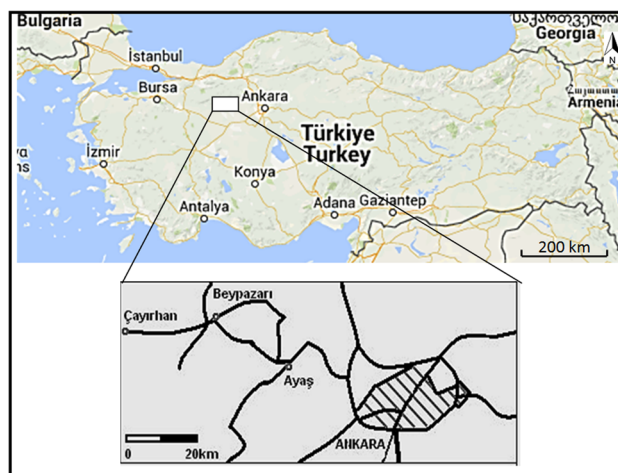


Fig. 1 Location map of Cayirhan Underground Lignite Mine

The Cayirhan coal basin is formed by an old miocene series called M1, M2, M3, and M4 and Pliocene formation (Fig. 2). Coal seams are located in the M1 formation, which is some four kilometers wide, and approximately 25 km long elongated in a south-west to north-east direction. There is a light brown colored limestone layer of 5–6 m over the coal seams and 7–8 m green colored claystone layer below the seams. Under clay-stone there is a 15–20 m thick layer of volcanic breccia. Also, a third coal seam is found 140–160 m below the workable seams. The M2 formation consists of clay and marl at a thickness of 80–120 m. There are two bituminous schist layers of 20 m at the top and bottom. M3 is the hardest formation composed of beige colored siliceous limestone and having a thickness about 30–35 m. This is the major aquifer zone in the field. Many cavities and fractures at the bottom levels are enabling collection of water. The majority of the area is covered with the M4 formation composed of grey, red, green, and beige tuffs. Despite their hard structure, they break into parts when subjected to water. Therefore, 15–20 cm of clastic portions covers the surface. The thickness of this formation is about 80 m and consists of silica of 5–10 cm at the bottom layers. The two main normal faults, Davutoglan fault and North fault, in the

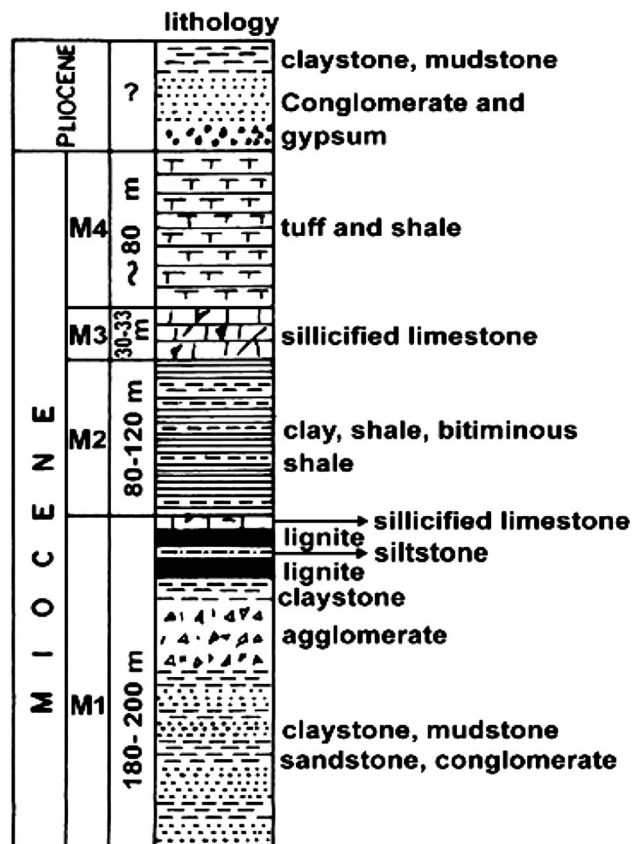


Fig. 2 Vertical cross-section (Aydin and Funfstuck 1988)

north-west and south-east directions, are almost parallel and about 1.5–2 km apart from each other (Haciosmanoglu 2004).

## Field studies

A Dosco Mk-2B roadheader with a 112 kW cutter head power was observed during roadway construction in rock (Fig. 3). The machine has a conical cutterhead with unequal circumferential pick spacing. The longitudinal (axial) cutter head has a diameter of about 600 mm and fitted with 24 point attack picks (Fig. 4). The general data of the machine is given in Table 1.

The cutting times of the machine were recorded at eight different locations. The volume of the material cut for each location was calculated by using the cross-sectional area and the depth of cut. Then, the ICR values were calculated



Fig. 3 Dosco Mk-2B roadheader



Fig. 4 The cutter head of Dosco Mk-2B roadheader

**Table 1** Technical data for Dosco Mk-2B roadheader

General data	
Dimensions (length, height, width)	10.2 × 2.0 × 3.0 m
Maximum cutting height	5.4 m
Total power	224 kW
Total weight	44 ton
Head drive power	112 kW
Maximum walking speed	8.4 m/min
Maximum operating slope	14°

by dividing the volume of the material cut by cutting time (Table 1).

Any joint system was not observed at the locations of performance measurements. Because the strata thickness is larger than the tunnel height, any bedding plane was not also observed. The type of material and some properties are given in Table 2. A photo of a measurement and sampling location is also shown in Fig. 5.

Large block samples of rock were also collected from each test location for experimental studies. Each block sample was inspected for macroscopic defects so that it would provide test specimens free from fractures, partings, or alteration zones.

## Laboratory studies

When a roadheader pick is forced into the rock, a highly stressed zone is produced under the pick tip. As the pick is kept pressed into the rock, pick forces exceed the strength of the material and material is cracked. The principle failure mechanism is considered to be predominantly tensile for brittle rock, with shear failure applying to plastic rocks (Fowel 1993; Tiryaki and Dikmen 2006). Because the most effective rock parameter in rock cutting with a pick is the tensile strength, the Brazilian tensile strength test and point load strength test, which is a form of indirect tensile test, were selected for this study. The block punch

**Fig. 5** The photo of a measurement and sampling location

strength is also a measure of tensile strength (Sulukcu and Ulusay 2001).

In addition to strength properties, the mineralogical and petrographic properties of rock also affect the breakage (Fowel 1993; Tiryaki and Dikmen 2006). In this context, porosity is selected. Ultrasonic velocity, density, and water absorption are closely related to porosity and reflect mineralogical structure of rock.

Core samples were prepared from the block samples collected from the site. ASTM (1984) standards or ISRM (2007) suggested methods were followed during the testing. The applied methods in the tests are briefly described in the following. The summaries of the test results are presented in Table 3. The number of specimen tested is limited for some tests, because some of the weak samples were disintegrated or broken during sample preparation.

## Brazilian tensile strength test

Brazilian tensile strength tests were performed on core samples having a diameter of 38 mm and a height to diameter ratio of 0.5–1.0. Both ends of core were cut parallel and placed between the standard loading jaws. The jaws were placed between the loading frames of the point

**Table 2** Measurement and sampling locations, and the type of material

Location code	Locations	Material	Material properties
1	G 4007-2.1 Main incline, m.356	Limestone	Massive
2	D 110 Tailgate, m.512	Clayey limestone	Massive, partly clayey filling
3	D 110 Tailgate, m.80	Limestone	Massive
4	D 110 Tailgate, m.538	Clayey limestone	Massive, partly clayey filling
5	D 110 Tailgate, m.570	Clayey limestone	Clayey filling
6	D 110 Tailgate, m.525	Clayey limestone	Clayey filling
7	D 110 Tailgate, m.548	Clayey limestone	Clayey filling
8	D 110 Tailgate, m.323	Clayey limestone	Clayey filling

**Table 3** Instantaneous cutting rates and the average results of tests

Location code	ICR (m <sup>3</sup> /h)	BTS (MPa)			$I_s$ (MPa)			$V_p$ (km/s)		
		Min.	Max.	Aver.	Min.	Max.	Aver.	Min.	Max.	Aver.
1	12.5	1.17 (6)*	2.05	1.67 ± 0.35**	0.73 (7)	0.92	0.81 ± 0.07	1.63 (3)	1.79	1.69 ± 0.08
2	12.9	1.50 (7)	3.61	2.92 ± 0.75	1.02 (7)	1.69	1.36 ± 0.26	2.17 (3)	2.32	2.22 ± 0.07
3	8.6	9.40 (8)	12.27	10.85 ± 0.91	2.95 (7)	3.72	3.38 ± 0.35	2.33 (3)	2.66	2.52 ± 0.14
4	10.3	2.45 (6)	3.56	2.94 ± 0.37	0.80 (8)	0.96	0.90 ± 0.06	2.02 (3)	2.03	2.02 ± 0.01
5	6.5	1.80 (6)	2.31	2.01 ± 0.20	0.48 (7)	0.81	0.69 ± 0.12	1.77 (3)	1.86	1.81 ± 0.04
6	10.5	1.85 (6)	2.06	2.05 ± 0.18	0.53 (8)	0.79	0.62 ± 0.10	2.01 (3)	2.02	2.01 ± 0.01
7	12.6	7.77 (7)	10.43	9.39 ± 0.92	1.99 (7)	3.09	2.61 ± 0.43	2.48 (3)	2.78	2.68 ± 0.14
8	10.9	4.82 (7)	7.53	6.22 ± 0.98	1.74 (8)	2.57	2.10 ± 0.38	2.33 (3)	2.75	2.59 ± 0.19

Location code	ICR (m <sup>3</sup> /h)	BPI (MPa)			$\rho$ (g/cm <sup>3</sup> )			$n$ (%)			$A_w$ (%)		
		Min.	Max.	Aver.	Min.	Max.	Aver.	Min.	Max.	Aver.	Min.	Max.	Aver.
1	12.5	2.64 (5)	4.82	3.11 ± 0.92	2.16 (3)	2.27	2.20 ± 0.06	18.7 (3)	22.2	20.5 ± 2.5	8.8 (3)	11.5	10.0 ± 1.1
2	12.9	5.15 (4)	6.84	5.91 ± 0.70	2.05 (3)	2.14	2.11 ± 0.05	15.9 (3)	17.3	16.8 ± 0.7	7.7 (3)	8.9	8.3 ± 0.8
3	8.6	8.01 (5)	10.13	9.21 ± 0.87	2.06 (3)	2.34	2.22 ± 0.14	9.6 (3)	13.1	12.0 ± 1.8	4.6 (3)	6.3	5.4 ± 0.9
4	10.3	2.63 (5)	5.19	4.01 ± 0.90	1.68 (3)	1.70	1.69 ± 0.01	24.8 (3)	25.8	25.4 ± 0.5	13.8 (3)	16.6	15.2 ± 1.0
5	6.5	1.47 (5)	3.30	2.55 ± 0.61	1.69 (3)	1.71	1.70 ± 0.01	26.2 (3)	28.0	27.2 ± 0.9	15.2 (3)	16.9	16.3 ± 0.9
6	10.5	3.94 (4)	5.25	4.52 ± 0.58	2.00 (3)	2.02	2.01 ± 0.01	23.6 (3)	25.7	24.3 ± 1.2	11.8 (3)	14.2	12.9 ± 1.2
7	12.6	9.48 (5)	12.16	10.52 ± 1.00	2.25 (3)	2.38	2.33 ± 0.07	5.6 (3)	8.3	7.6 ± 1.5	2.6 (3)	4.5	3.4 ± 0.9
8	10.9	6.11 (4)	6.96	6.37 ± 0.34	2.16 (3)	2.27	2.22 ± 0.06	15.0 (3)	18.3	16.8 ± 1.7	5.9 (3)	8.0	7.4 ± 1.0

\* Number test

\*\* Standard deviation

load apparatus by using flat platens. A spherical loading head is also placed over the upper jaw. A tensile loading rate of about 200 N/s was applied until failure occurred. Performing the Brazilian tensile test and some samples after testing is shown in Fig. 6. At least six samples were tested for each rock type, and the results were averaged as Brazilian tensile strength (BTS).

### Point load strength test

The samples cored perpendicular to any visible weakness plane and the samples having weakness plane were discarded. The axial point load tests were carried out on the cores having a diameter of 38 mm and a thickness of 15 mm (Fig. 7). Because the sample preparation is crucial in the axial point load test, the test specimens were cut parallel by using an automatic core cutting machine. After placing specimens between the conical platens of the device, the load is steadily increased such that failure occurs within 10–60 s. The testing device and some of tested samples are indicated in Fig. 7. The calculated test results were corrected to a specimen diameter of 50 mm. The tests were repeated at least seven times for each rock type, and the average value was recorded as the point load strength ( $I_s$ ).

### Block punch strength test

The 42 mm-diameter core samples having thicknesses between 6 and 10 mm were used in the block punch strength tests. Disc specimens were cut parallel by using an automatic core cutting machine. After removing the conical platens, block punch apparatus was mounted onto the ram of the point load device. Then, the specimen was centered on the base support of the test apparatus and clamped. The load was gradually applied to the specimens at a constant rate such that failure occurred within 10–60 s. Figure 8 shows the testing and some of the failed samples after test. The tests were repeated at least four times for each rock type and the average value was taken as the block punch index (BPI) value.

### Ultrasonic velocity test

P-wave velocities were measured on the samples having a diameter of 38 mm and a length of approximately 40 mm. ISRM (2007) recommends the minimum lateral dimension to be not less than ten times the wavelength. In this study, because the transducers have high frequency, the wavelength is very small and the lateral dimensions of the specimens are in acceptable limits. Another important

**Fig. 6** Carrying out the Brazilian tensile test using point load apparatus (a) and some samples after testing (b)

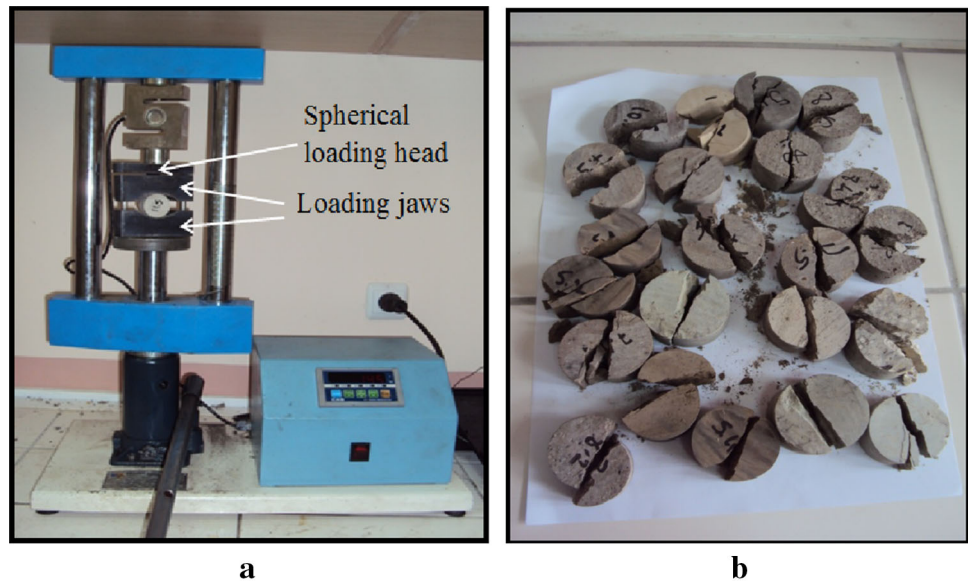
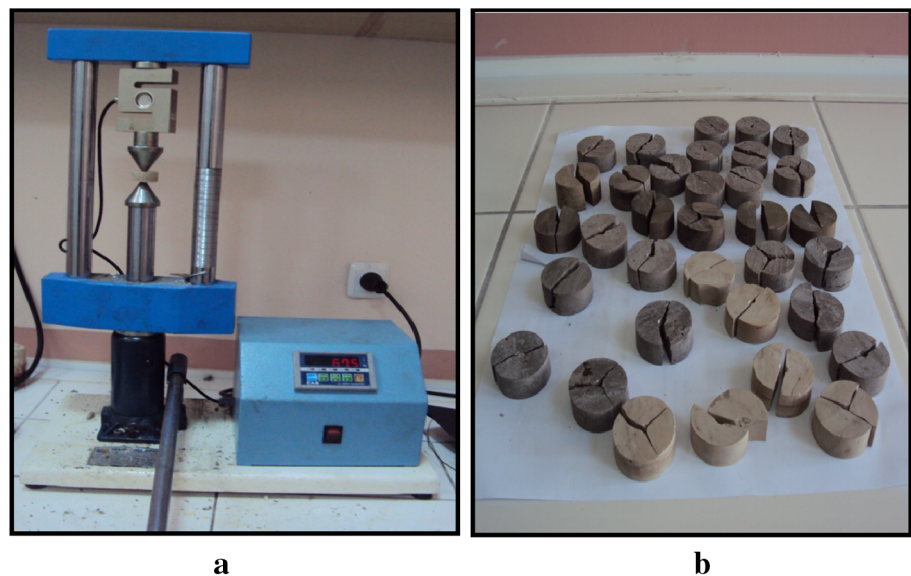


**Fig. 7** Point load testing (a) and some samples after testing (b)



factor affecting the ultrasonic velocity is the grain size of the rock tested. ISRM (2007) also recommends that the travel distance of the pulse through the rock shall be at least ten times the average grain size. Since the tested rocks have a very small grain sizes, the travel distance of the pulse satisfies the suggested methods.

End surfaces of the core samples were polished sufficiently smooth to provide good coupling. In the tests, the PUNDIT 6 instrument and two transducers (a transmitter and a receiver) having a frequency of 1 MHz were used (Fig. 9). A good acoustic coupling between transducer faces and sample surface is necessary for the accuracy of a transit time measurement. Stiffer grease was used as a coupling agent in this study. Transducers were pressed to

either end of the sample, and the pulse transit time was recorded. The tests were repeated three times for each rock type and the average value was taken as the P-wave velocity ( $V_p$ ) value.

#### Density ( $\rho$ ) test

Smooth-cut core samples were used in the determination of air-dried density. The specimen volume was calculated from the average of several calliper readings. The mass of the specimen was determined by a balance, capable of weighing to an accuracy of 0.01 of the sample mass. The density values were obtained from the ratio of the specimen mass to the specimen volume. At least three samples

**Fig. 8** Carrying out the block punch test using point load apparatus (a) and some samples after testing (b)

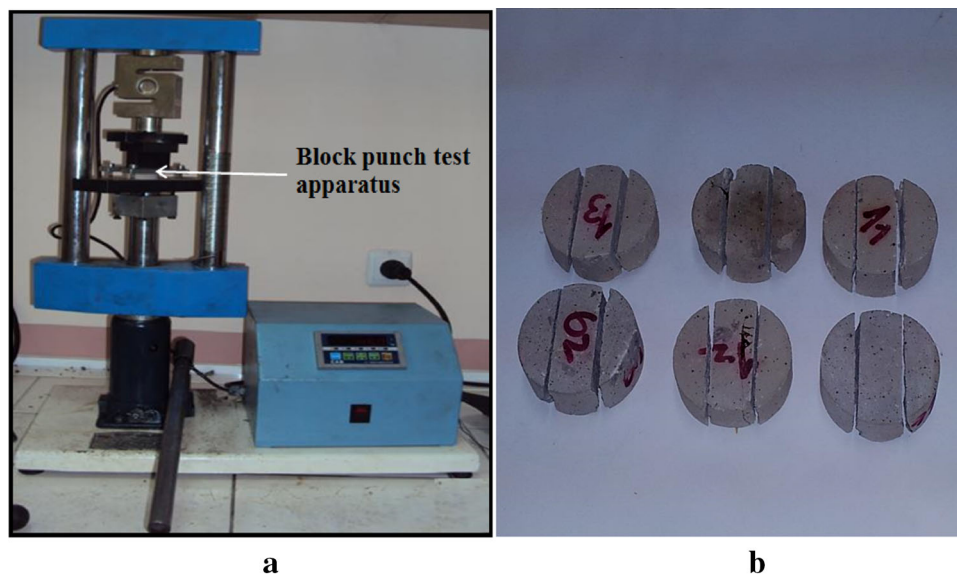


**Fig. 9** Ultrasonic velocity test

were tested for each rock type, and the results were averaged.

### Porosity ( $n$ ) test

Porosity values were determined using the saturation and calliper techniques. Pore volumes were calculated from the dry and saturated mass, and sample volumes were obtained from calliper readings. The porosity values were obtained from the ratio of the pore volumes to the specimen volume. The test was repeated at least three times for each rock type, and the results were averaged.

### Water absorption by weight ( $A_w$ )

The saturated masses of core samples were determined after 24 h of immersion in water. Then, the samples were

dried for 24 h, and the dry masses of samples were measured. The water absorption by weight values were calculated from the mass of water absorbed by the rock divided by its oven-dried mass and expressed as a percentage. The test was repeated at least three times for each rock type and the results were averaged.

### Evaluation of the results

As shown in Table 3, the BTS values range from 1.67 to 10.85 MPa. The  $I_s$  values range from 0.62 to 3.38 MPa. The  $V_p$  values range from 1.69 to 2.68 km/s. The BPI values range from 2.55 to 10.52 MPa. The density values range from 1.69 to 2.33 g/cm<sup>3</sup>. The porosity values range from 7.57 to 27.21 %. The water absorption by weight values range from 3.37 to 16.33 %. The test results have a wide range in respect to establish some correlations. In order to compare the test result with the published data, a literature review was done. However, only one unpublished study (Keles 2005) was found. This material included BTS test results performed on the two different clayey limestones in the Cayirhan Coal Mine. The BTS values are 6.2 and 6.8 MPa. As stated above, the BTS values in this study vary from 1.67 to 10.85 MPa.

The histogram plots of the test values were investigated, and it was shown that the values generally have a non-normal distribution. While some test values are skewed to the right hand, the others are skewed to the left.

The cross-correlation was also carried out to show the correlation coefficients among the all variables of the test values. As shown in Table 4, there is a high correlation between the variables except for density.



**Table 4** The cross-correlation between the test results

	BTS (MPa)	$I_s$ (MPa)	$V_p$ (km/s)	BPI (MPa)	$\rho$ (g/cm <sup>3</sup> )	$n$ (%)	$A_w$ (%)
BTS (MPa)	1.00						
$I_s$ (MPa)	0.98	1.00					
$V_p$ (km/s)	0.87	0.87	1.00				
BPI (MPa)	0.93	0.91	0.92	1.00			
$\rho$ (g/cm <sup>3</sup> )	0.60	0.66	0.61	0.71	1.00		
$n$ (%)	-0.85	-0.87	-0.83	-0.94	-0.86	1.00	
$A_w$ (%)	-0.80	-0.84	-0.80	-0.89	-0.93	0.98	1.00

**Simple regression analysis**

The ICR values measured in the field and rock properties were analyzed using the method of least squares regression. The BTS,  $I_s$ ,  $V_p$ , BPI,  $\rho$ ,  $n$ , and  $A_w$  values were correlated with the ICR values. Linear, logarithmic, exponential, and power curve fitting approximations were executed to check if there are some correlations between the ICR values and rock properties. As shown in Figs. 10, 11, 12, and 13, there are no correlations between the ICR values and the BTS,  $I_s$ ,  $V_p$ , BPI. On the other hand, weak correlations exist between the ICR values and  $\rho$ ,  $n$ , and  $A_w$  values (Figs. 14, 15, 16). Normally it is expected that there is an inverse relation between the ICR values and  $\rho$  because increasing density generally increases the rock strength. That the correlation is inverse may be due to the some other factors affecting the ICR values. On the other hand, the relations between the ICR values and  $n$  and  $A_w$  values should normally be proportional since increasing  $n$  and  $A_w$  values generally decreases the rock strength. However, the ICR value does not depend on only one rock property. For this reason, in order to obtain a reliable estimation equation for the prediction of the ICR, multiple regression analysis should be performed.

**Stepwise multiple regression analysis**

Stepwise multiple regression analysis was carried out for the derivation of the best model to predict the ICR of roadheaders. The  $I_s$  and water absorption by weight were

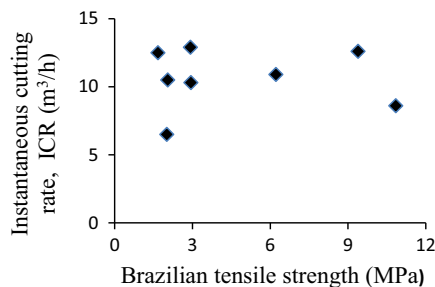


**Fig. 10** The relation between ICR and Brazilian tensile strength

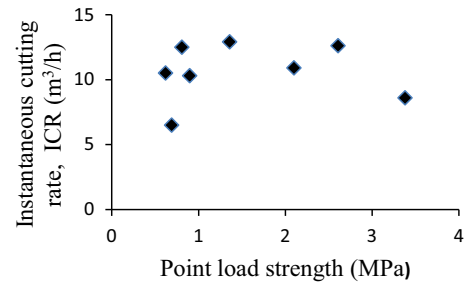


**Fig. 11** The relation between ICR and point load strength

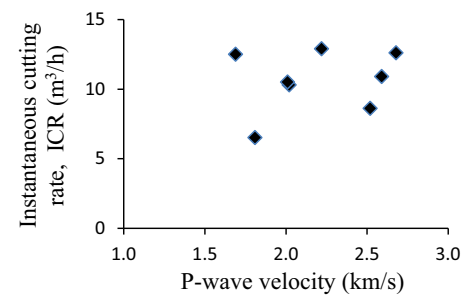


**Fig. 12** The relation between ICR and P-wave velocity

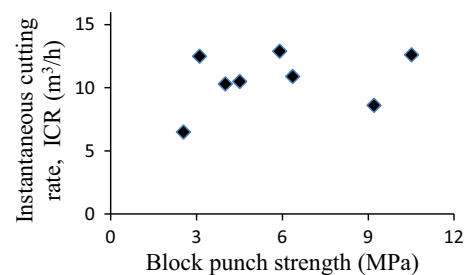


**Fig. 13** The relation between ICR and block punch strength

included for the best model. The best model is given as follows:

$$ICR = -2.92I_s - 0.79A_w + 22.95 \quad r = 0.89. \quad (15)$$

Alternative simple models including two variables were also derived for practical usage. Significant models among these models can be alternatively used where the Eq. (15)

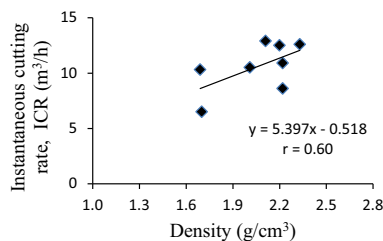


Fig. 14 The relation between ICR and density

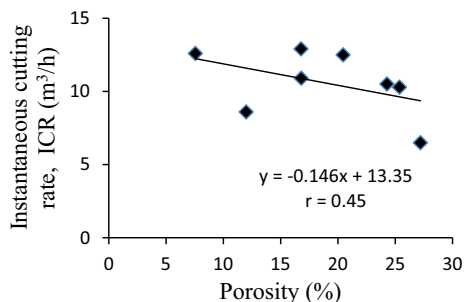


Fig. 15 The relation between ICR and porosity

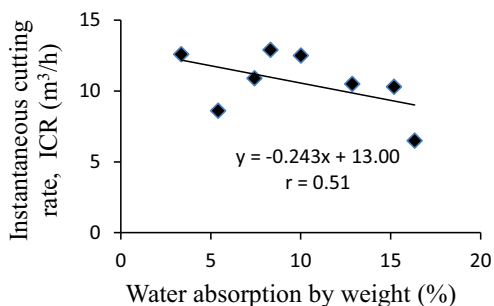


Fig. 16 The relation between ICR and water absorption by weight

cannot be used. The derived alternative models are the following:

$$ICR = -0.88\sigma_t - 0.54n + 25.01 \quad r = 0.88, \quad (16)$$

$$ICR = -3.23I_s - 0.57n + 26.35 \quad r = 0.86, \quad (17)$$

$$ICR = -1.02BPI - 0.55n + 26.74 \quad r = 0.64, \quad (18)$$

$$ICR = -3.21V_p - 0.29n + 23.11 \quad r = 0.55, \quad (19)$$

$$ICR = -0.72\sigma_t - 0.69A_w + 20.86 \quad r = 0.87, \quad (20)$$

$$ICR = -0.70BPI - 0.63A_w + 20.81 \quad r = 0.65, \quad (21)$$

$$ICR = -3.41V_p - 0.46A_w + 22.65 \quad r = 0.62, \quad (22)$$

$$ICR = -0.35\sigma_t + 8.58\rho - 5.39 \quad r = 0.76, \quad (23)$$

$$ICR = -1.34I_s + 9.10\rho - 6.07 \quad r = 0.76, \quad (24)$$

$$ICR = -0.23BPI + 7.32\rho - 3.14 \quad r = 0.63, \quad (25)$$

$$ICR = -1.52V_p + 6.83\rho - 0.12 \quad r = 0.63, \quad (26)$$

where,  $\sigma_t$  is the Brazilian tensile strength (MPa),  $I_s$  is the point load strength (MPa), BPI is the block punch strength (MPa),  $V_p$  is the ultrasonic velocity (km/s),  $\rho$  is density ( $g/cm^3$ ),  $n$  is porosity (%), and  $A_w$  is the water absorption by weight (%).

### Validation of the derived models

The correlation coefficients of some equations derived are good or very good, but they do not necessarily identify a valid model. The validation of the Eqs. (15, 16, 17, 20, 23, 24) was checked by the  $F$  test.

The significance of the regressions was determined by the analysis of variance. In this test, a 95 % level of confidence was chosen. If the computed  $F$  value is greater than the tabulated  $F$  value, the null hypothesis is rejected so that there is a real relation between the dependent and independent variables. The computed  $F$  values are greater than the tabulated  $F$  values for all equations except the Eqs. (23, 24) as shown in Table 5. Therefore, it is concluded that all equations except the Eqs. (23, 24) are valid according to the  $F$  test.

### Discussion

As shown above, there are no correlations between the ICR values and rock properties. This is an expected result, because the excavation rate of a mechanical excavator is not only one rock property. After examining the derived equations, it can be stated that the first controlling parameters of the ICR are the strength parameters such as  $BTS$  and  $I_s$ . The second controlling parameters are density, porosity, and water absorption. The other controlling parameter is probably the clay contents of the content of the rocks under investigation. The clay contents of the tested rocks could not be determined, but the water absorption ratios were measured. The water absorption ratio is an indicator of clay content. It is known that increasing clay content generally increases the water absorption ratio (Ward et al. 2005; Zhang et al. 2012). The clay content of rock can significantly affect the performance of roadheaders in wet conditions. Bilgin et al.

Table 5  $F$  test results

Equation no	$F$ table	$F$ test
15	5.99	9.91
16	5.99	8.91
17	5.99	7.43
20	5.99	7.79
23	5.99	3.35
24	5.99	3.43

(2004) reported that the ICR of roadheaders decreased from 50 to 20 m<sup>3</sup>/h in a sticky (muddy) clayey zone. Thuro and Plinninger (1998) showed that the roadheader performance generally decreases with increasing percentage of clay and silt. In wet conditions, clayey rocks sticks to the cutting head, hence, decreases the ICR value. On the other hand, clayey rocks form mud with water and cannot be removed by the haulage system of a roadheader. Therefore, the performance of a roadheader is defeated by mucking problems. Similar problems were observed during the field studies of this research. The sticking of clay onto the cutterhead caused a decrease in the ICR values. Although the rock under excavation had low strength, low ICR values were measured at some locations, compared to the locations having similar strength. For example, although the tensile strength of rock is very low (2.01 MPa), the ICR value is not high (6.5 m<sup>3</sup>/h) for the measurement location 5. The clay problem was also observed during the performance measurement at this location. The water absorption value of the rock at this location is also high (% 16.3), which is an indication of high clay content. On the other hand, the tensile strength of rock is very low (2.92 MPa) and the ICR value is high (12.9 m<sup>3</sup>/h) for the measurement location 2. At this location, the water absorption value of the rock is low (% 8.3). That water absorption ratio is included in the best model (Eq. 15) is probably an indicator of the controlling effect of clay content.

Figure 16 shows the correlation between the ICR and water absorption. Although the correlation coefficient weak, there is an inverse correlation between the two parameters. Increasing water absorption decreases the ICR. That the correlation coefficient is weak is probably due the fact that the other rock properties affect the correlation. It was observed at the some measurement locations that clayey rocks stuck to the cutter head and decreased the ICR and also stuck to the haulage system of the roadheader.

The joint conditions of rock mass may affect significantly the performance of roadheaders. Thuro and Plinninger (1998) showed that the roadheader performance increases with decreasing joint spacing for the joints having a spacing of less than 63 mm. Bilgin et al. (2004) stated that discontinuity spacing smaller than around 10 cm increases the instantaneous cutting rate. Some researchers (Bilgin et al. 1990; Ebrahimabadi et al. 2011; Abdolreza and Yakhchali 2013) included the rock quality designation (RQD) in their performance prediction models for roadheaders. Bilgin et al. (2000) and Balci and Bilgin (2001) stated that ground stresses and rock discontinuities should be taken into account for the performance prediction of roadheaders and suggested the following equation:

$$\text{ICR} = k \frac{P}{\text{SE} \times k_1 \times k_2}, \quad (27)$$

where ICR is the instantaneous cutting rate (m<sup>3</sup>/h),  $P$  is the cutting head power (kW or HP),  $k$  is the energy transfer ratio (0.85–0.90 for TBMs and 0.45–0.55 for roadheaders),  $\text{SE}$  is the specific energy (kWh/m<sup>3</sup>),  $k_1$  is the correction factor for ground stress ( $\approx 1.3$  for considerable stress), and  $k_2$  is the correction factor for geological discontinuities (0.5 for RQD = 20–30 % and 0.7 for RQD = 30–50 %).

Because any significant joint system was not observed at the locations of performance measurements in this study, the effect of jointing could not be included in the analysis. However, in the case of discontinuity, a correction can be made by dividing the ICR values calculated by using the equations derived in this study by the correction factors ( $k_1$  and  $k_2$ ) for geological discontinuities.

## Conclusions

The performance prediction for roadheaders was investigated by using easy testing methods such as Brazilian tensile strength, point load strength, block punch strength, ultrasonic velocity, density, porosity, and water absorption ratio. Simple and multiple regression analysis were carried out to develop performance prediction models for the instantaneous cutting rates (ICR) of roadheaders. Any significant correlation was not found between the ICR and the physico-mechanical rock properties. Then, stepwise multiple regression analysis was performed, and the best model was selected for the estimation of the ICR. The best model includes point load strength and water absorption by weight and has a very good correlation coefficient ( $r = 0.89$ ). In order to present alternative choices for the practitioners, simple models including two variables were also derived.

The derived models do not include the joint condition of the rock mass, since any significant joint system was not observed at the locations of performance measurements. A correction method for the models was suggested for the geological discontinuities.

In addition to correlation coefficients, the validity of the derived models was checked by the  $F$  test. It was concluded that the developed models, which are statistically significant, could be practically used for the performance prediction of roadheaders with the same or very similar cutterhead power and similar cutterhead design, which are used in similar formations. That the models have easy testing methods will be an advantage when using them. Because the first author works in the coal mine under investigation, he observed later the performance of the machine and validated the findings of this study.

The finding of this study indicates that simple regression analysis by including one rock property is inadequate for the

performance prediction of roadheaders. The microstructural properties such as porosity and water absorption, and clay contents of rocks to be excavated have important effects of the ICR of roadheaders. Further research is necessary to investigate in detail the effects of clay content of formations on the performance of roadheaders.

## References

- Abdolreza YC, Yakhchali SH (2013) A new model to predict roadheader performance using rock mass properties. *J Coal Sci Eng* 19(1):51–56
- Altindag R (2003) Correlation of specific energy with rock brittleness concepts on rock cutting. *J S Afr Inst Min Metall* 103:163–171
- ASTM (1984) American Society for Testing and Materials. Standard test method for unconfined compressive strength of intact rock core specimens. *Soil and Rock, Building Stones: Annual Book of ASTM Standards 4.08*. ASTM, Philadelphia, Pennsylvania
- Aydin Y, Funfstuck J (1988) Bey pazari project report. In: Proceedings of the sixth coal congress of Turkey. Chamber of Mining Engineers of Turkey, pp 53–71 (**in Turkish**)
- Balci C, Bilgin N (2001) Estimating the specific energy from rock properties for selection of rapid excavation system. In: Proceedings 10th international symposium mine planning equipment selection, New Delhi, India, November 19–21, pp 393–400
- Balci C, Demircin MA, Copur H, Tuncdemir H (2004) Estimation of optimum specific energy based on rock properties for assessment of roadheader performance. *J S Afr Inst Min Metall* 11:633–641
- Bilgin N, Seyrek T, Erdinc E, Shahriar K (1990) Roadheaders clean valuable tips for Istanbul Metro. *Tunn Tunn* 22:29–32
- Bilgin N, Tuncdemir H, Balci C, Copur H, Eskikaya S (2000) A model to predict the performance of tunnelling machines under stressed condition. AITES-ITA2000 World Tunnel Congress, Durban. South African Institute of Mining and Metallurgy, pp 47–53
- Bilgin N, Dincer T, Copur H, Erdogan M (2004) Some geological and geotechnical factors affecting the performance of a roadheader in an inclined tunnel. *Tunn Undergr Sp Tech* 19:629–636
- Comakli R, Kahraman S, Balci C (2014) Performance prediction of roadheaders in metallic ore excavation. *Tunn Undergr Sp Tech* 40:38–45
- Copur H, Ozdemir L, Rostami J (1998) Roadheader applications in mining and tunneling industries. In: Annual meeting of American society for mining, metallurgy and exploration (SME), Orlando, Florida, March 10–12, Preprint Number: 98–185
- Copur H, Tuncdemir H, Bilgin N, Dincer T (2001) Specific energy as a criterion for the use of rapid excavation systems in Turkish Mines. *Trans Inst Min Metall (Sect A Min Technol)* 110:A149–A157
- Ebrahimabadi A, Goshtasbi K, Shahriar K, Seifabad MC (2011) A model to predict the performance of roadheaders based on rock mass brittleness index. *J S Afr Inst Min Metall* 111(5):355–364
- Fowel RJ (1993) The mechanics of rock cutting. In: Hudson JA (ed) *Comprehensive rock engineering*, vol 4. Pergamon Press, Oxford, Seoul, Tokyo, pp 155–176
- Gehring KH (1989) A cutting comparison. *Tunn Tunn* 21:27–30
- Goktan RM (1991) Brittleness and micro-scale rock cutting efficiency. *Min Sci Technol* 13:237–241
- Haciosmanoglu ME (2004). Development of a subsidence model for Cayirhan coal mine. MSc. Thesis, Middle East Technical University, p 154
- ISRM (2007) The complete ISRM suggested methods for rock characterization, testing and monitoring: 1974–2006. Suggested methods prepared by the commission on testing methods, international society for rock mechanics. In: Ulusay R, Hudson JA (eds) *Compilation arranged by the ISRM Turkish national group*, Ankara, Turkey, Kozan Ofset
- Keles S (2005) Cutting performance assessment of a medium weight roadheader at Cayirhan coal mine. MSc. Thesis. Middle East Technical University (**unpublished**)
- McFeat-Smith I, Fowell RJ (1979) The selection and application of roadheaders for rock tunnelling. In: Maevis AC, Hustrulid WA (eds) *Proc., rapid excavation and tunnelling conference*. AIME, Atlanta, pp 261–279
- Ocak I, Bilgin N (2010) Comparative studies on the performance of a roadheader, impact hammer and drilling and blasting method in the excavation of metro station tunnels in Istanbul. *Tunn Undergr Sp Tech* 25:181–187
- Rostami J, Ozdemir L, Neil DM (1994) Performance prediction: a key issue in mechanical hard rock mining. *Min Eng* 4:1263–1267
- Singh SP (1987) Criterion for the assessment of the cuttability of coal. *Undergr Min Methods Technol* 8:225–239
- Sulukcu S, Ulusay R (2001) Evaluation of the block punch index test with prime consideration on size effect, failure mechanism and its effectiveness in predicting rock strength. *Int J Rock Mech Min Sci* 38(8):1091–1111
- Thuro K, Plinninger RJ (1998) Geological limits in roadheader excavation—four case studies. In: The 8th International IAEG Congress, pp 3545–3552
- Thuro K, Plinninger RJ (1999) Roadheader excavation performance—geological and geotechnical influences. In: The 9th ISRM congress, theme 3: rock dynamics and tectonophysics/rock cutting and drilling, Paris, pp 1241–1244
- Tiryaki B, Dikmen AC (2006) Effects of rock properties on specific cutting energy in linear cutting of sandstones by picks. *Rock Mech Rock Eng* 39(2):89–120
- Tumac D, Bilgin N, Feridunoglu C, Ergin H (2007) Estimation of rock cuttability from shore hardness and compressive strength properties. *Rock Mech Rock Eng* 40(5):477–490
- Ward CR, Nunt-jaruwong S, Swanson J (2005) Use of mineralogical analysis in geotechnical assessment of rock strata for coal mining. *Int J Coal Geol* 64:156–171
- Zhang N, He M, Liu P (2012) Water vapor sorption and its mechanical effect on clay-bearing conglomerates selected from China. *Eng Geol* 141–142:1–8